



# Preclinical Characterization of GST-HG141, a Novel Hepatitis B Virus Capsid Assembly Modulator

Dong Zhang<sup>1\*</sup>, Wenqiang Wu<sup>1\*</sup>, John Mao<sup>1\*</sup>, Zhigan Jiang<sup>3\*</sup>, Vadim Bichko<sup>1</sup>, Qiaoyun Zhou<sup>2</sup>, Jing Wang<sup>3</sup>, Jian Li<sup>3</sup>, Shuhui Chen<sup>3</sup>, Haiying He<sup>3\*</sup>, and George Zhang<sup>1\*</sup>

<sup>1</sup>Fujian Akeylink Biotechnology Co., Ltd., Shanghai, China

<sup>2</sup>Fujian Cosunter Pharmaceutical Co., Ltd., Fuzhou, China

<sup>3</sup>Domestic Discovery Service Unit, WuXi AppTec (Shanghai) Co., Ltd. Shanghai, China

## Abstract

HBV Capsid Assembly Modulators (CAMs) had emerged as promising oral agents for Anti-Hepatitis B Virus (HBV) drug development, with a potential for Chronic Hepatitis B (CHB) functional cure. Here we report the discovery and preclinical characterization of GST-HG141, a novel HBV CAM, currently under phase II clinical evaluation in CHB patients. In vitro, GST-HG141 induced HBV core protein assembly and the formation of intact capsids without affecting capsid morphology. GST-HG141 potently inhibited HBV DNA secretion in HepG2 2.15 cells, and was additive with nucleos(t)ide analogs, but with no shift from T = 4 towards T = 3 capsid formation in contrast to other CAM-Es. Furthermore, GST-HG141 retained potent antiviral activity against HBV genotypes A-D, and against nucleos(t)ide- and CAM-resistant mutants, but with significantly different resistance profile from other CAMs. In the HBV-infected Primary Human Hepatocytes (PHH), GST-HG141 inhibited de novo synthesis of the HBV cccDNA, but had no effect on the established cccDNA pools. Finally, in an AAV/HBV mouse model in vivo, GST-HG141 robustly and dose-dependently reduced serum (~3.0 log<sub>10</sub>) and liver (0.9 log<sub>10</sub>) HBV DNA with no significant effect on body weight. Our data demonstrate that GST-HG141 acts on different steps of the HBV life cycle, consistent with the CAM-E MOA, but its exact MOA and resistance profile appears to be distinct from other CAM-Es and CAM-As reported in the literature. GST-HG141 has since completed Ph1a clinical study in healthy subjects (NCT04386915) (9), and demonstrated robust antiviral efficacy in a 28-day Ph1b study in CHB patients (NCT04868981) (data will be reported elsewhere). Further clinical evaluation of GST-HG141 is ongoing.

**Keywords:** Hepatitis B Virus; Capsid Assembly Modulator; GST-HG141; cccDNA

## Introduction

Despite wide availability of safe, effective and inexpensive vaccines, hepatitis B infections remain a major global health problem. Over 2 billion people globally have serologic evidence of the past or present HBV infection, and approximately 296 million people currently have Chronic Hepatitis B (CHB) [1]. Chronic Hepatitis B (CHB) often leads to cirrhosis, liver failure, or hepatocellular carcinoma [2]. Current standard of care options, Nucleos(t)ide Analogues (NA) and PEGylated interferons [2-4] seldom lead to a functional CHB cure, defined as sustained loss of hepatitis B surface antigen (HBsAg) and undetectable serum HBV DNA for 6 months off treatment, with or without HBsAg seroconversion [5]. Thus, novel therapeutic approaches with different Mechanisms of Action (MOAs) are urgently needed to combat CHB.

The HBV core protein (HBcAg) plays a key role in multiple steps of HBV life cycle. A correct HBcAg self-assembly into viral capsids, containing virus genomes, is indispensable for HBV replication [6,7]. The

capsid assembly process has recently emerged as an important target for the treatment of chronic hepatitis B. Several Capsid Assembly Modulators (CAMs) have been reported and some are under clinical evaluations for CHB functional cure [8].

Here we report the discovery and pre-clinical characterization of GST-HG141, a novel, potent and selective HBV CAM, which has a distinct molecular mechanism of its antiviral action compared to other CAMs reported in the literature, and has demonstrated strong antiviral properties in pre-clinical studies in vitro and in vivo. GST-HG141 has since completed a phase 1a study in healthy subjects, and a 28-day phase 1b study in CHB patients. GST-HG141 demonstrated good safety, tolerability, and PK properties in healthy volunteers in the Ph1a study (NCT04386915) [9]. In the phase 1b study in CHB patients [10], GST-HG141 demonstrated significantly more potent antiviral activity in CHB patients than other direct anti-viral agents (DAAs) currently used or in clinical development. In this 28-day multi-center, randomized, double-blind, placebo-controlled phase 1b study (NCT04868981), the treatment of GST-HG141 at 50 and 100 mg doses led to a rapid and robust decline in serum HBV DNA in CHB patients (mean reduction values of 2.9 log<sub>10</sub> IU/ml and 3.4 log<sub>10</sub> IU/ml, respectively [10]. GST-HG141 is currently under investigation in a Ph2 study in CHB patients (NCT05637541).

## Materials and Methods

### Compounds

All compounds used in this study were synthesized by WuXi AppTech (Shanghai, China) with > 99% purity.

### Fluorescence Quenching Assay

The purified recombinant c-terminally truncated HBV core protein Cp150 was prepared as previously described [12,13]. The Cp150 protein was labeled with maleimidyl BoDIPY-FL at the c-terminal amino acid residue. The Cp150 protein and serial dilutions of test compounds were added to black view, flat-bottom plates and assembly was induced by adding NaCl. The fluorescent signal (extinction: 480 nm; emission: 540 nm; instrument: Enzyme Calibration (Molecule Device, SpetraMax M2),

**Submitted:** 12 April, 2024 | **Accepted:** 23 April, 2024 | **Published:** 25 April, 2024

\***Corresponding author(s):** George Zhang, Fujian Akeylink Biotechnology Co., Ltd., Shanghai, China

**Haiying He**, Domestic Discovery Service Unit, WuXi AppTec (Shanghai) Co., Ltd. Shanghai, China

#These authors contributed equally to this work.

**Copyright:** © 2024 Zhang G, He H, et al., This is an open-access article distributed under the terms of the Creative Commons Attribution License, which permits unrestricted use, distribution, and reproduction in any medium, provided the original author and source are credited.

**Citation:** Zhang G, He H, Zhang D, Wu W, Mao J, et al. (2024) Preclinical Characterization of GST-HG141, a Novel Hepatitis B Virus Capsid Assembly Modulator. SM J Infect Dis 7: 11.



Hitrap Desalting columns (5 ml, GE Biosciences, 17-1408-1), Nanodrop (Thermo, Nanodrop 2000) was measured every 10 sec for 30 min, and the  $EC_{50}$  values were calculated.

### Size Exclusion Chromatography

The Cp150 protein was incubated with 30  $\mu$ M GST-HG141, BAY41-4109 or 0.5% DMSO (untreated control) for 24 h in the presence of 150 mM NaCl, and separated using size exclusion chromatography. The elution profiles were quantified by absorbance at 280 nm (mAU, milli-absorbance units). Samples were run sequentially on the same Superdex 200 column using ÄKTA™ pure - Cytiva System under identical conditions.

### Electron Microscopy

The Cp150 protein dimers preparation was treated with compounds as describes for SEC above. The final DMSO concentration in the re-assembly mix was 0.2%. Same DMSO concentration was used as a negative control. Samples were adsorbed for 5 minutes to the glow discharged Formvar/carbon film-coated 400 mesh copper grids, washed with water three times, stained 1 minute with 2% uranyl acetate in water, blotted on Whatman 1 filter paper and air-dried. Images were collected with the Jeol 1400 plus microscope at 80 kV with a bottom mounted Gatan one view camera.

### Antiviral Assay in HepG2.2.15 Cells and Cytotoxicity Assay

The antiviral activity of GST-HG141 and reference compounds on HBV DNA in HepG2.2.15 cells was assessed by qPCR assay. On day 1, test compounds were first diluted with DMSO (from 500 nM to 0.076 nM at 3-fold dilutions), and further diluted with medium to reach final concentration; and the final volume per well was 200  $\mu$ l. The final concentration of DMSO in the culture medium was 0.5%. The compounds were tested with 9 concentrations in triplicate.

HepG2.2.15 cell were seeded in 96-well plates at the density of  $4.0 \times 10^4$  cells/well (0.1 ml/well) on Day 0. The cells were cultured at 37°C and 5% CO<sub>2</sub> for 3 days. On day 4, the plates were refreshed with culture media containing compounds. On day 7, culture supernatants were collected for DNA isolation. After collection of supernatants, Cell Titer-Glo reagent was added to the assay plates. The plates were incubated at room temperature for 10 min. Luminescence signal were read the by BioTek-Synergy 2. Extracellular DNA was isolated with QIAamp 96 DNA Blood Kit per the manufacturer's manual. A plasmid containing the HBV full-genome sequence (D type) is used as a standard sample for HBV DNA quantification. The range of the standard used is between 101 -  $1.0 \times 10^7$  copies/ $\mu$ l. The PCR is performed with 95°C for 10 min, then cycling at 95°C for 15 sec, 60°C for 1 min for 40 cycles. The assays were performed three times, and the  $EC_{50}$  were analyzed and obtained using GraphPad Prism.

The cytotoxicity in HepG2.2.15 and several other mammalian cell lines and primary cells (MRC-5, HEK293, Caki-1, HepG2, MT-4, Colo-205, H1 HeLa, A375, Hep2, Huh7 and CCRF-CEM) were assessed using CellTiter-Glo (CTG) assay kit from Promega (G7573). The compounds were diluted 3-fold with DMSO for 8 times from the starting concentration of 50  $\mu$ M to have a concentration range from 50  $\mu$ M to 0.0076  $\mu$ M. The cells were seeded in a 96-well plate at a density between 5000 to 10,000 cells per well. The cells were incubated at 37°C with the compounds for 72 hrs before CTG assays were performed. The plates were assessed and analyzed by BioTek, Synergy 2.

### Antiviral Assays with other Viruses

The antiviral activities of GST-HG141 and reference compounds (GS-7977, Acyclovir, VX-787) on several other representative DNA and RNA viruses including HCV (plus strand RNA virus), replicon GT1b (from Wuxi AppTec) in Huh7 cells, Herpes simplex virus (HSV-1) (DNA virus), GHSV-UL46 (from ATCC, VR-1544) in Vero cells, and Influenza virus

(minus strand RNA virus), A/PR/8/34 (H1N1) from ATCC (VR-1469) in MDCK cells were assessed after the infected cells were incubated with the compounds at 37°C for 5 days. The cell viability was assessed using assay kits Cell Titer-fluor (Promega, G6082) or CCK8 (Lee Shanghai, D3100L4057). The  $EC_{50}$  and  $CC_{50}$  were analyzed and obtained using GraphPad Prism.

### Compound Treatment and Assays in HBV Infected Primary Human Hepatocytes (PHHs)

Cryopreserved Primary Human Hepatocytes (PHH) from an individual donor were obtained from WuXi Apptech (Cat. No. M00995-P). The cells infected with HepAD38-derived HBV virions were treated with HBV inhibitors in two different schemes, Scheme I -starting the treatment at the time of HBV infection (Day 0), and Scheme II -starting the treatment at Day 5 post-infection. The cells were treated by compounds at various concentrations using serial dilutions ranging from 10  $\mu$ M to 0.08  $\mu$ M and incubated for 1 hour at room temperature. Approximately 24 hours after plating in collagen coated 96-well plates (Thermo Fisher Scientific; CM1096) at a density of 55,000 to 75,000 live PHH cells per well, medium was removed and HepAD38-derived HBV virions in the presence of compounds were transferred from v-shaped 96-well plates to PHH-containing 96-well plates in triplicate wells for each compound concentration before removing remaining extracellular virions by washing with fresh medium 3 times. Maintenance media with or without test compounds were replenished every 3-4 days post-infection. At the end of the treatment, the supernatant was collected, cell debris was removed, and cells were washed once and lysed. After 10 min at room temperature, cells were collected and centrifuged, and the cell lysate was stored. HBV particles were precipitated from cell culture supernatants, and the resulting pellet was incubated overnight to dissolve the viral particles. Cell lysates and dissolved virus particle samples were subjected to Southern blotting to detect HBV DNA according to the method described below.

### Detection of HBV Capsids by Western Blot

For Western blotting, intra- and extracellular HBV particles were resolved on a 1% agarose gel and transferred to a nitrocellulose membrane. After fixation and blocking, membranes were incubated with a polyclonal rabbit HBV core antibody (DAKO) followed by an anti-rabbit horseradish peroxidase-linked antibody (Amersham/GE Healthcare) in blocking buffer. Washed membranes were treated with SuperSignal west femto maximum-sensitivity substrate according to the manufacturer's instructions (Thermo Fisher Scientific) and imaged with an ImageQuant LAS 4000.

### Hirt-Extracted DNA from HBV-infected PHHs and Southern Blotting

Extraction of covalently closed circular DNA was conducted by the Hirt method. In brief, covalently closed circular (cccDNA) extracts were resolved on an agarose gel. DNA was transferred from the gel to a nylon membrane overnight, after UV crosslinking, hybridization was carried out (EasyHyb ready-to-use buffer with a DIG-labeled HBV probe). The DIG-labeled probe was detected using a DIG luminescent detection kit (Roche) according to the manufacturer's instructions. Visualization of hybridization signals was achieved with a chemiluminescent substrate, and the light signal produced was captured with an ImageQuant LAS 4000.

### Measurement of HBeAg and HBsAg Concentrations by ELISA Immunoassay

Extracellular hepatitis B virus S antigen (HBsAg) and hepatitis B virus E antigen (HBeAg) were detected in culture media by an electrochemiluminescence assay (MSD) as previously reported.



## Immunofluorescence Microscopy

HepAD38 cells, harbouring an integrated over-the-length HBV genomic DNA were treated with serial 10-fold dilutions (0.01 - 10  $\mu\text{M}$ ) of HBV inhibitors for 3 days, fixed and blocked as described in Supplementary Materials. Cell monolayers were incubated with anti-HBc mab (clone C1, ABCAM ab8637), followed by goat anti-mouse IgG (H+L) cross-adsorbed Alexa Fluor 488 secondary antibody (Invitrogen A-11001) for 1 hour. After the wash step as above, cells were visualized using an inverted immunofluorescent microscope (Supplementary Methods).

## AAV/HBV Mouse Model

In this study, the AAV/HBV mouse model was used to evaluate the *in vivo* anti-HBV efficacy of compound GST-HG141 and its synergistic effect with TDF. Male C57BL / 6 mice were injected with AAV / HBV (genotype D) through the tail vein, and the drug was started four weeks later. The vehicle, the test compound GST-HG141 and the control compound TDF were given by continuous intragastric administration for 28 days. Among them, the vehicle and the test compound GST-HG141 were administered twice a day, the dosage of GST-HG141 was 10, 30 and 100 mg / kg; the control compound TDF was administered once a day, the dosage was 1 mg / kg ; And for GST-HG141 and TDF co-administration group, the dosage is 10 mg / kg and 1 mg / kg, respectively. During the experiment, blood samples of mice were collected to collect serum; on days 28 and 42 of the experiment, several groups of mice were sacrificed to collect serum and liver tissue samples, respectively. The *in vivo* anti-HBV drug efficacy of the compound was evaluated by quantitatively detecting the content of HBV DNA, HBV RNA in serum samples and HBV DNA in liver.

## Pharmacokinetic Studies

To evaluate pharmacokinetics of GST-HG141, the mice plasma samples from the AAV/HBV model study were collected before and after the last dosing at Day 27. Blood samples were collected at 0 h (before dosing), 1 h, 4 h, 8 h, 9 h, 12 h, and 24 h from the group of GST-HG141 treatment at 10 mg/kg, BID. The blood samples were prepared using K2EDTA, plasma samples separated by centrifugation at 7,000 g, and analyzed by liquid chromatography-tandem mass spectrometry (LC/MS) to determine plasma concentrations of the compound. Pharmacokinetic parameters, including area under the plasma concentration-time curve from time 0 to 24 hour (AUC<sub>tau</sub>), maximal concentration (C<sub>max</sub>) and concentration at 24 hours following last dose (C<sub>tau</sub>) were determined by non-compartmental analysis using Phoenix WinNonlin 6.4 (Pharsight Corporation, Princeton, NJ).

## Results

### Biochemical Characterization of GST-HG141

In order to determine the effect of GST-HG141 on HBV capsid assembly *in vitro*, the biochemical quenching assay [11] was used. The purified recombinant c-terminally truncated HBV core protein Cp150 [12,13] was labeled with maleimidyl BoDIPY-FL at the c-terminal amino acid residue and the assembly was induced with NaCl, with or without serial dilutions of GST-HG141 or GLS4, a known CAM as a reference [14], as described in Materials and Methods. The fluorescent signal (extinction: 480 nm; emission: 540 nm) was measured every 10 sec for 30 min, and the EC<sub>50</sub> values were calculated. In this assay, GST-HG141 accelerated HBV core protein assembly (Table 1), with the EC<sub>50</sub> value of 0.93  $\pm$  0.11  $\mu\text{M}$  (Mean  $\pm$  SD). A similar effect was observed with the reference CAM GLS4 (EC<sub>50</sub> = 3.34  $\pm$  0.47  $\mu\text{M}$ ), consistent with its mechanism of action [14,15]. This observation confirmed that GST-HG141 is a CAM.

Next, the Size Exclusion Chromatography (SEC) studies were performed. BAY41-4109, a known CAM-A (11, 15), was used as a reference compound. The Cp150 protein was incubated with 30  $\mu\text{M}$  GST-HG141, 30  $\mu\text{M}$  BAY41-4109 or 0.5% DMSO (untreated control) for

24 h in the presence of 150 mM NaCl, and separated using size exclusion chromatography on the Superdex 200 column. After DMSO treatment, HBV capsids (first peak) and core protein dimers (second peak) eluted at the expected retention times (Figure 1). Compound GST-HG141 did not significantly change the retention time of the intact capsids (first peak), indicating its CAM-E MOA, while BAY41-4109 (a known CAM-A), altered (shortened) the retention time of the first peak, as expected, suggesting formation of larger core protein aggregates.

**Table 1:** Effect of GST-HG141 and GLS4 on HBV capsid assembly in biochemical quenching assay *in vitro*.

Compound	EC <sub>50</sub> ( $\mu\text{M}$ )			
	Exp. 1	Exp. 2	Exp. 3	Mean $\pm$ SD
GLS4	3.75	2.85	3.45	3.34 $\pm$ 0.47
GST-HG141	1.02	0.98	0.81	0.93 $\pm$ 0.11

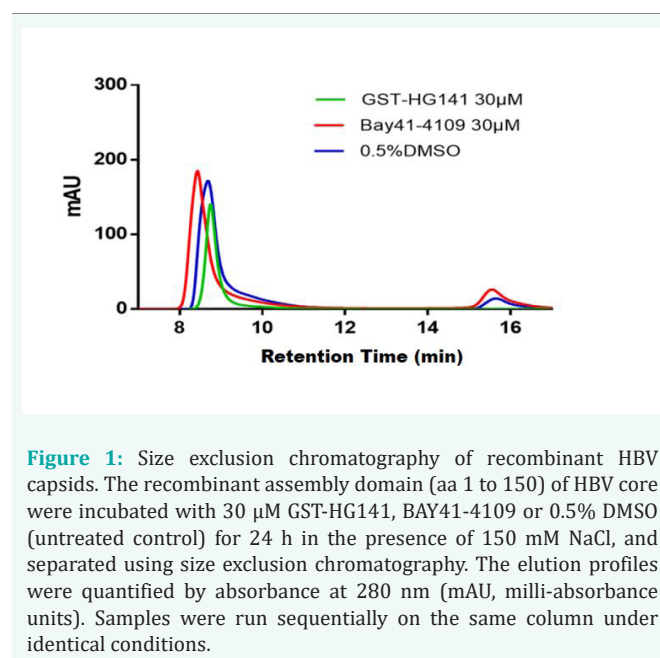


**Figure 1:** Size exclusion chromatography of recombinant HBV capsids. The recombinant assembly domain (aa 1 to 150) of HBV core were incubated with 30  $\mu\text{M}$  GST-HG141, BAY41-4109 or 0.5% DMSO (untreated control) for 24 h in the presence of 150 mM NaCl, and separated using size exclusion chromatography. The elution profiles were quantified by absorbance at 280 nm (mAU, milli-absorbance units). Samples were run sequentially on the same column under identical conditions.

These findings were further confirmed by the Transmission Electron Microscopy (TEM). The HBV core protein Cp150 samples were obtained as for the SEC studies above, except compound GLS4 was used as a reference CAM. The Cp150 protein dimers preparation was treated with compounds as describes for SEC above. The final DMSO concentration in the re-assembly mix was 0.2%. Same DMSO concentration was used as a negative (untreated) control. Samples were adsorbed for 5 min to Formvar/carbon film-coated 400 mesh copper grids, washed and stained with 2% uranyl acetate in water as described in Materials and Methods. Images were collected with the Jeol 1400 plus microscope at 80 kV with a bottom mounted Gatan one view camera. Compound GST-HG141 treatment did not cause apparent changes in capsid size or morphology (Figure 2), consistent with its CAM-E MOA. Treatment with GLS4 led to formation of aberrant HBcAg structures, in accordance with its known MOA as a CAM-A.

### *In vitro* Antiviral Activity of GST-HG141 in Cellular Assays

GST-HG141 potently inhibited secretion of HBV DNA in HepG2.2.15 cells, stably replicating HBV. The 50% Effective Concentration (EC<sub>50</sub>) value of GST-HG141 in this assay was 8.2  $\pm$  3.7 nM, similar to that of GLS4,



a reference CAM, and TDF ( $11.9 \pm 4.5$  and  $6.2 \pm 1.2$  nM, respectively) (Table 2). No cytotoxicity was observed for neither compound ( $CC_{50} > 50 \mu\text{M}$ ). Similarly, GST-HG141 was not cytotoxic in MRC-5, HEK293, Caki-1, HepG2, MT-4, Colo-205, H1 HeLa, A375, Hep2 and Huh7 cell lines (data not shown). To evaluate the effect of GST-HG141 on different HBV genotypes, GST-HG141 was tested in HepG2 cells transiently-transfected with HBV isolates from genotypes A-D, and GST-HG141 demonstrated potent inhibitions on these various HBV genotypes with the  $EC_{50}$  values ranging from 26 to 228 nM (Table 3). GST-HG141 also retained potency against a number of major known CAM- and nucleos(t)ide-resistant mutants (Table 4). The antiviral activity of GST-HG141 was HBV-specific, as several other representative DNA and RNA (plus- or minus-strand) viruses were not inhibited in the cellular assays *in vitro* (Data not shown).

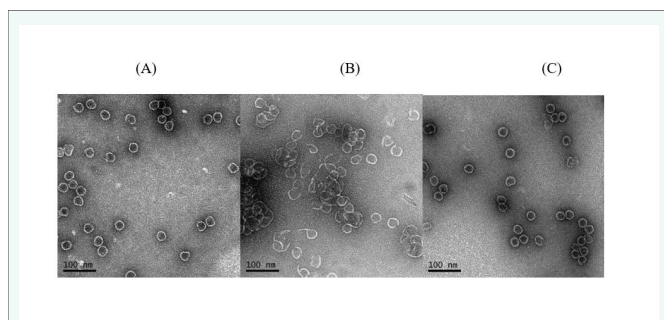


**Figure 2:** TEM images of the *in-vitro*-assembled purified recombinant HBcAg domain (aa 1-150), treated with DMSO (A), 20  $\mu\text{M}$  GLS-4 (B), or 20  $\mu\text{M}$  GST-HG141 (C).

**Table 2:** The effect of GST-HG141 on the secretion of HBV DNA in HepG2.2.15 cells. The experiment was repeated three times, and the average  $EC_{50}$  values are shown

Compound	$EC_{50}$ (nM)
GST-HG141	$8.16 \pm 3.65$
GLS4	$11.89 \pm 4.50$
TDF	$6.16 \pm 1.21$

**Table 3:** Inhibition of secreted HBV DNA of different genotypes in transiently-transfected HepG2 cells. The  $EC_{50}$  values from a typical experiment are shown, as well as accession numbers of the HBV genomes used

HBV isolate (genotype)	$EC_{50}$ , nM						
	AP007263 (A)	HE974371 (A)	AB246345 (C)	AB246346 (C)	JN406371 (B)	AB033554 (B)	U95551 (D)
GST-HG141	59	33	26	32	41	47	228
ETV	0.3	1.9	1.1	2.3	1.3	1.5	1.0

The antiviral effect of GST-HG141 in combination with nucleos(t)ides (TDF, ETV), was studied in the HepG2.2.15 cells, using the Bliss-Independence model (Prichard) and MacSynergy II software. In these experiments, GST-HG141 in combination with TDF or ETV acted in an additive manner (Data not shown). No cytotoxicity was observed with any of the drugs or drug combinations tested. To assess antiviral effect of GST-HG141 in Primary Human Hepatocytes (PHHs) infected with HBV, the cells were treated with HBV inhibitors in two different schemes, Scheme I - starting treatment at the time (Day 0) of HBV infection, and Scheme II - starting treatment at Day 5 post-infection. Supernatant samples were collected on Day 1 or Day 6 post-infection for Scheme I and Scheme II, respectively. Extracellular HBV DNA was measured by qPCR, HBeAg and HBsAg by ELISA and intracellular HBV cccDNA by Southern

**Table 4:** Antiviral potency against nucleos(t)ide and CAM resistance mutants. The mean  $EC_{50}$  fold shift values, compared to those of the WT virus, are shown. ND, not determined.

HBV Mutant	GST-HG141	GLS-4	AT-130	ETV
WT (U95551)	1	1	1	1
Core F23Y	4.8	2	18	1
Core P25G	1.2	13	13	0.8
Core T33N	7	98	49	0.9
Core T109M	23	1.7	3.6	0.4
Core V124F	70	63	1.2	0.5
Pol M204I+S202G	0.7	ND	ND	4913
Pol M204I+S202G+M250V	1	ND	ND	3956

blot, respectively (Figure 3-5 and Table 5). The identity of the cccDNA band was confirmed by heat denaturation, with or without a subsequent EcoR I digestion, as shown in (Figure 4C). After heat denaturation at 88°C for 8 min, cccDNA band migration was unchanged. However, after EcoRI digestion, with or without heat denaturation, HBV DNA species migrated as  $\sim 3.2$  kb linear double-stranded DNA.

In this study, reference compounds ETV and GLS4 showed expected antiviral activity against HBV. Specifically, GLS4 showed dose-dependent inhibitory effect on extracellular HBV DNA for both Scheme I and Scheme II, and inhibited extracellular HBeAg, HBsAg and intracellular HBV cccDNA for Scheme I. However, GLS4 had no obvious reduction of extracellular HBeAg, HBsAg, and intracellular cccDNA for Scheme II (Figure 3A,3B, Figure 4A,4B, Table 5). ETV (5  $\mu\text{M}$ ) potently inhibited extracellular HBV DNA for both schemes, but had no significant activity against extracellular HBeAg, HBsAg intracellular cccDNA for either treatment scheme (Data not shown). Similarly to GLS4, GST-HG141 concentration-dependently inhibited the extracellular HBV DNA for both Scheme I and Scheme II. It also inhibited extracellular HBeAg, HBsAg and intracellular HBV cccDNA for Scheme I, but not for Scheme II (Figure 3A, 3B, Figure 4A, 4B, Table 5). No obvious cytotoxicity was observed for any of the compounds tested, as was determined by CCK-8 cell viability assay.

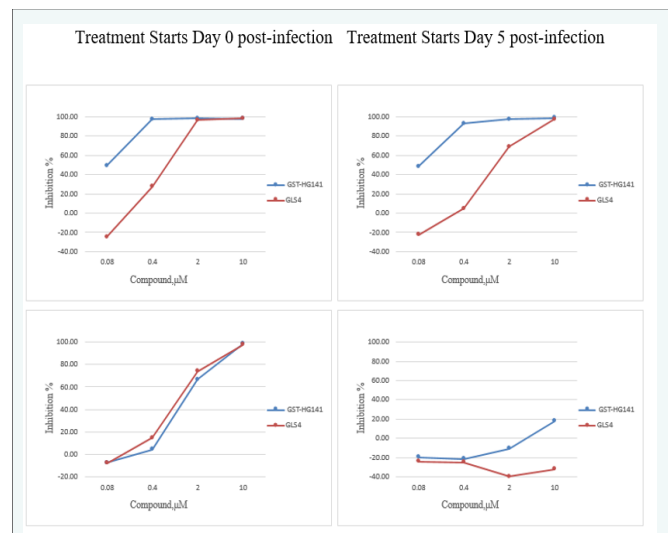


**Figure 3A:** Effect on secreted HBV DNA (top panel), and HBeAg (bottom panel) in HBV-infected PHH.

Treatment Starts Day 0 post-infection      Treatment Starts Day 5 post-infection

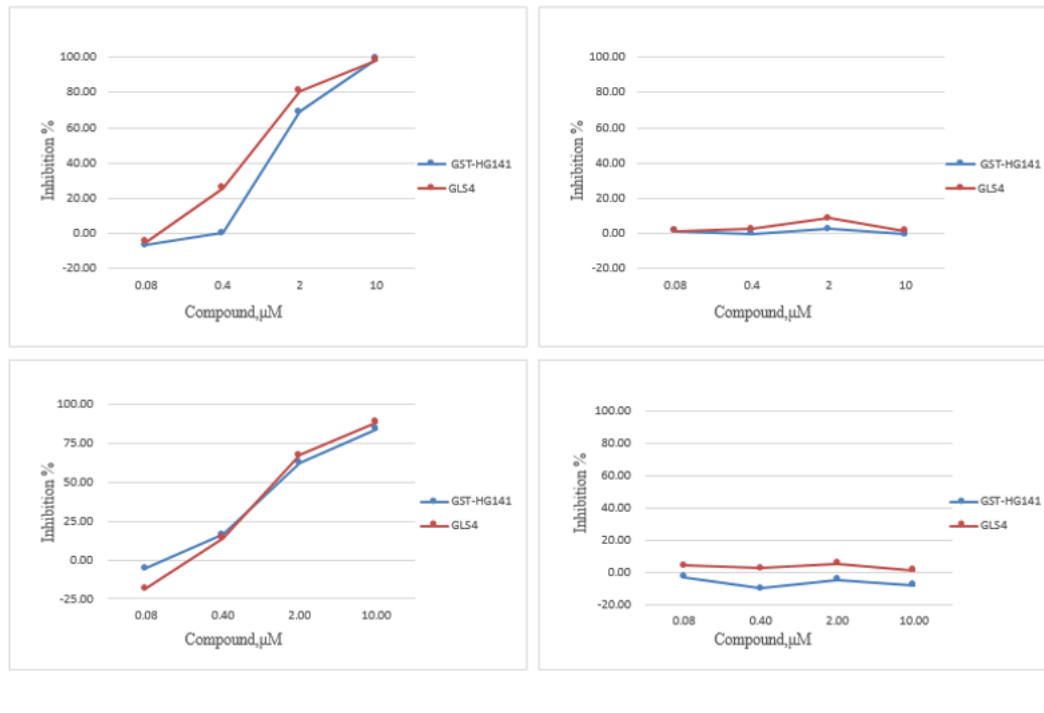


**Figure 3B** : Effect on secreted HBsAg (top panel), and intracellular cccDNA (bottom panel) in HBV-infected PHH.

**Figure 3**: Antiviral effects of GST-HG141 in HBV-infected Primary Human Hepatocytes (PHH). The PHH cells were treated with HBV inhibitors in two different schemes, Scheme I - starting treatment at the time (Day 0) of HBV infection, and Scheme II - starting treatment at Day 5 post-infection. Supernatant samples were collected 24 hr post-infection for Scheme I and Scheme II, respectively. Extracellular HBV DNA was measured by qPCR, HBeAg and HBsAg by ELISA and intracellular HBV cccDNA by Southern blot (Figure 4, Table 4), respectively. The results of a typical experiment are shown.

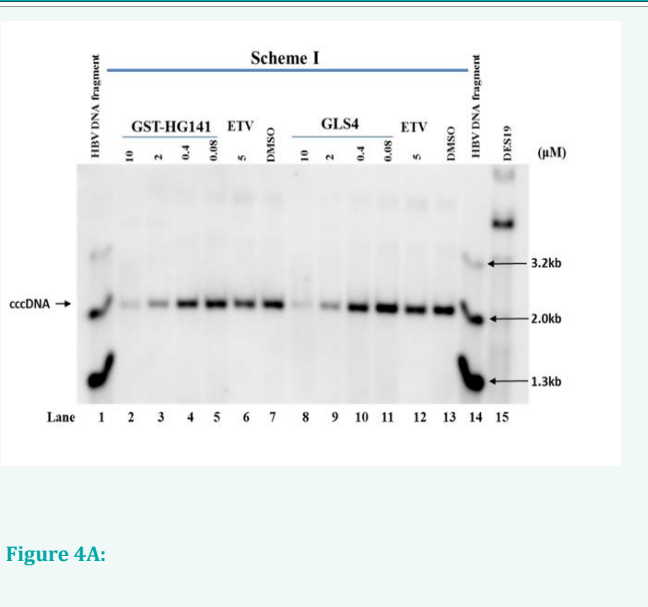


**Figure 4A:**

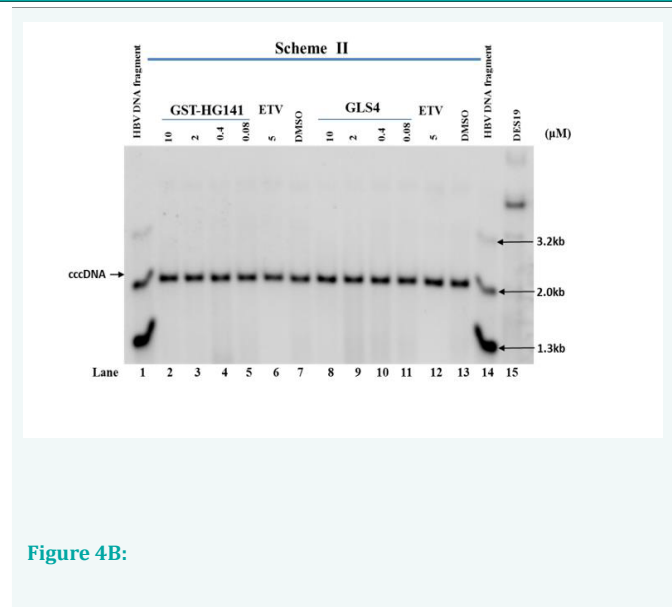


**Figure 4B:**



**Table 5:** Antiviral effect of GST-HG141 and GLS4 in HBV-infected primary human hepatocytes (PHHs).

Compound	HBV DNA	HBeAg	HBsAg	HBV cccDNA	Cytotoxicity	Treatment
	EC <sub>50</sub> (μM)				CC <sub>50</sub> (μM)	
<b>GST-HG141</b>	0.08	1.28	1.34	0.90	> 10	From day 0
<b>GLS4</b>	0.44	0.92	0.68	0.69	> 10	
<b>GST-HG141</b>	0.08	> 10	> 10	> 10	> 10	From day 5
<b>GLS4</b>	0.91	> 10	> 10	>10	> 10	

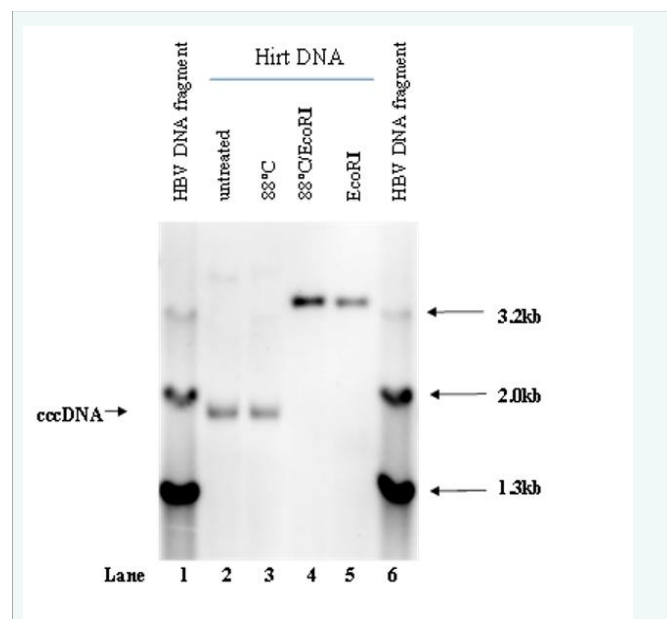


**Figure 4C:** Southern blot analysis of HBV cccDNA in HIRT DNA extracts from PHHs treated by GST-HG141, GLS4, and ETV. Cells were treated by Scheme I (4A) or Scheme II (4B) with GST-HG141 (lanes 2-5), GLS4 (lanes 8-11), 5 μM ETV (lanes 6 and 12), and DMSO (untreated control, lanes 7 and 13). Lane 15, Hirt DNA extract from DES19 cells. Fig.4C. Southern blot analysis of HBV cccDNA in HIRT DNA extracts from PHHs, untreated (lane 2), heat-denatured (lane 3), heat-denatured and digested with EcoRI (lane 4) or digested with EcoRI (lane 5). Lines 1 and 6, HBV DNA size markers.

### MOA Studies with GST-HG141 on Capsid Formation

To evaluate the mechanism of action of GST-HG141, the effect of GST-HG141 on encapsidated HBV DNA and RNA was tested in HepG2.1.15 cells. Following a 7-day treatment with various concentrations of GST-HG141, intracellular core particles were resolved by native high-concentration agarose gel electrophoresis, followed by Western, Southern- and Northern blotting with HBV-specific antibodies or probes (Materials and Methods). In these experiments, treatment with 0.01 and 0.1 μM GST-HG141 significantly reduced both HBV DNA and RNA content in the intracellular core particles (Figure 5). A dose-dependent increase in core particle formation was also observed with these drug concentrations. However, treatment with 1μM GST-HG141 led to capsid disruption and formation of larger, slower-migrating heterogenous HBcAg aggregates. No core particles were observed after treatment with GLS4, consistent with its CAM-A MOA. Treatment with AT-130 (a known CAM-E) led to a decrease in encapsidated DNA and RNA levels, and to an increase in capsid formation, consistent with its CAM-E MOA. A dose-dependent

shift from T = 4 capsids to T = 3 capsids was observed for AT-130, but not for GST-HG141 (Figure 5). These data indicate that treatment with GST-HG141 leads to the generation of HBV core capsids, devoid of viral DNA or pgRNA, consistent with its novel CAM-E MOA. Treatment with ETV led to a decrease in encapsidated viral DNA, but not RNA, consistent with ETV being a nucleoside inhibitor of reverse transcription by HBV polymerase. No effect on capsid formation was observed with ETV, as expected.

We next evaluated the effect of GST-HG141, GLS4 and AT-130 on the intracellular localization of the HBV core antigen (HBcAg) in cultured HepAD38 cells. Intracellular localization of HBcAg in Hep AD38 cells, treated with various concentrations of CAMs, was visualized using indirect immunofluorescence microscopy, as described in the Materials and Methods. Untreated HepAD38 cells demonstrated typical HBcAg localization: predominantly diffuse nuclear (nucleoplasm), but also diffuse cytoplasmic (Figure 6A). Treatment with 1 μM AT-130 (Figure 6B) led to a notable re-distribution of HBcAg from the nucleoplasm to the cytoplasm (diffuse cytoplasmic staining). In contrast, treatment with GLS4 led to redistribution of HBcAg within the nucleus: from the nucleoplasm (diffuse nuclear staining) to discrete nuclear domains (punctate nuclear pattern, Figure 6C). This effect was pronounced after treatment with as low as 0.01 μM GLS4 (not shown), and was enhanced further at 1 μM GLS4. The effect of GST-HG141 on the intracellular localization of HBcAg was similar to that observed with AT-130: re-localization from predominantly diffuse nuclear to predominantly diffuse cytoplasmic (Figure 6D). This effect was already visible with 0.01 μM GST-HG141, and was gradually enhanced with compound concentration increase up to 10 μM (not shown). Thus, GST-HG141 had a pronounced effect on the intracellular localization of HBcAg in HepAD38 cells, stably transfected with HBV genome, consistent with its CAM-E MOA.

### In Vivo Antiviral Efficacy of GST-HG141

The AAV / HBV mouse model was used to evaluate the in vivo anti-HBV efficacy of GST-HG141 alone or in combination with TDF. Male C57BL/6 mice were injected with AAV / HBV (genotype D) plasmid DNA and, after 4 weeks, animals were administered by oral gavage with various doses of vehicle (BID), GST-HG141 (BID), or TDF (QD). The HBV DNA and HBV RNA in serum, as well as HBV DNA in the liver, was quantitated by the real-time qPCR. Treatment with GST-HG141 alone significantly reduced HBV DNA levels in serum in a dose-dependent manner (Figure 7A). Serum HBV DNA was reduced by ~3.0 log<sub>10</sub> after 28 days treatment with 100 mg/kg GST-HG141. The HBV DNA levels in liver was also reduced significantly by GST-HG141 treatment (data not shown). A combination of GST-HG141 with TDF led to a greater reduction of the serum- and liver HBV DNA than either drug alone. The effect of GST-HG141 on the reduction of serum levels of HBV RNA was modest, but statistically significant. After 28 days of treatment with 100 mg/kg GST-HG141, average serum HBV RNA level was reduced by 1.09 log GE/ml (from 4.74 ± 0.08 to 3.64 ± 0.05 log GE/ml, *p* < 0.01). No significant changes in animal body weight dynamics, nor other signs of compound toxicity was observed in any of the animal treatment groups. On the 27th day of treatment, the average trough GST-HG141 plasma concentration was 78 nM (Figure 7B). The drug absorption peaked 1 hour after administration, the plasma half-life was 2.23 hours, and the AUC<sub>0-inf</sub> was 47600 nM.h (Table 6).

**Table 6:** Major PK parameters for GST-HG141 after 27 days of oral BID administration of 10 mg/kg to AAV/HBV mice.

<b>Cmax (nM)</b>	12200
<b>Tmax (h)</b>	1.00
<b>T<sub>1/2</sub> (h)</b>	2.23
<b>Tlast (h)</b>	24.0
<b>AUC<sub>0-last</sub> (nM.h)</b>	47300
<b>AUC<sub>0-8</sub> (nM.h)</b>	26000
<b>AUC<sub>0-inf</sub> (nM.h)</b>	47600
<b>MRT<sub>0-last</sub> (h)</b>	6.27
<b>MRT<sub>0-inf</sub> (h)</b>	6.36
<b>AUC<sub>0-inf</sub>/AUC<sub>0-last</sub> (%)</b>	101

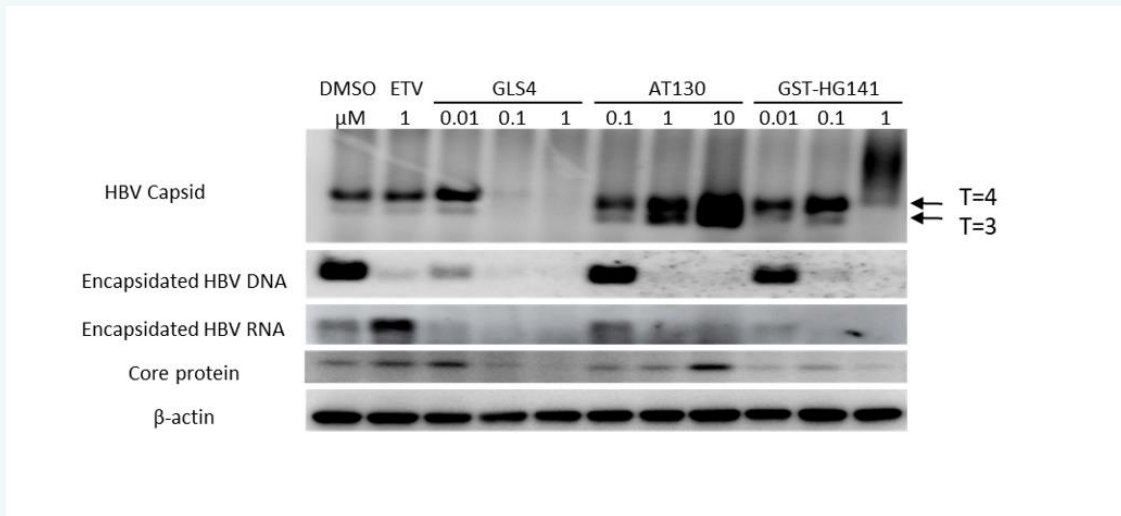


**Figure 5 :** Effect of GST-HG141 on the capsid-associated HBV DNA and RNA in HepG2.1.15 cells. After a 7-day treatment with various concentrations of GST-HG141, AT-130, GLS4, ETV, or DMSO control, intracellular core particles were resolved by native high-concentration agarose gel electrophoresis, followed by Western, Southern- and Northern blotting with HBV-specific antibodies or probes (Materials and Methods).

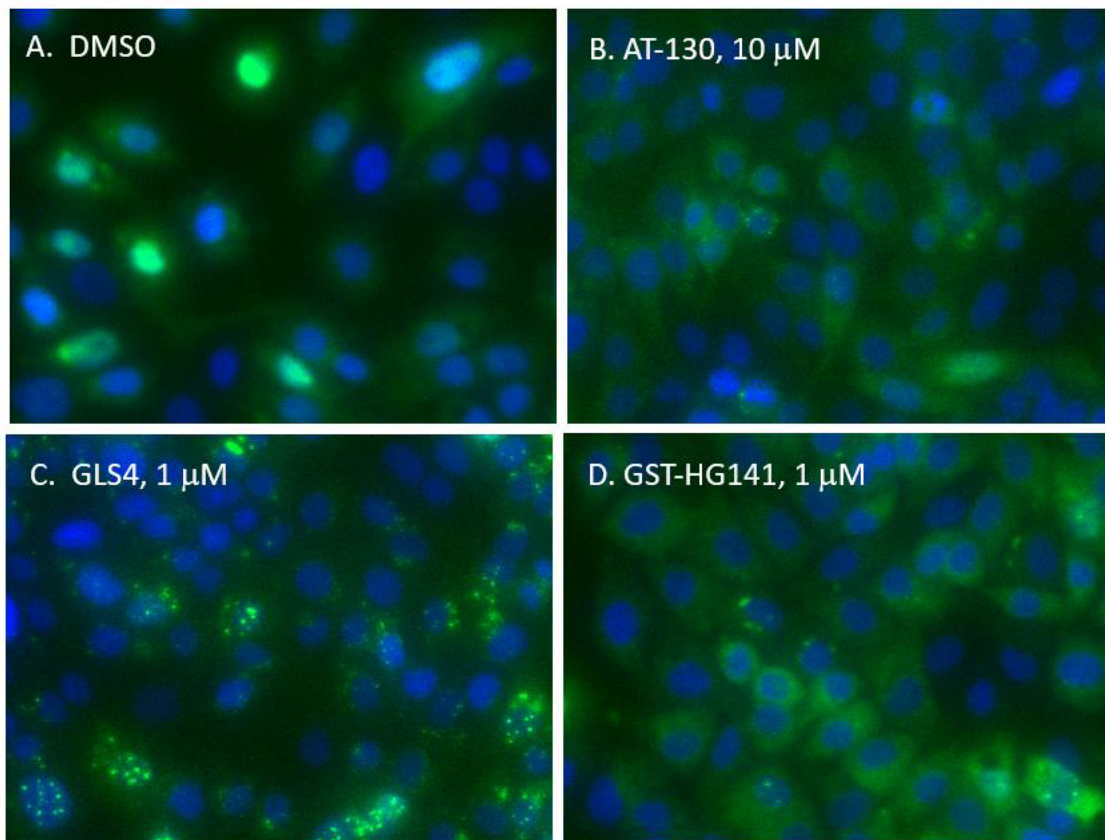


**Figure 6 :** Immunofluorescence assay of HepAD38 cells treated with different CAMs. Cells were cultured without tetracycline to induce HBV replication and with 0.01 -10 M of the respective test compound for 3 days. The HBCAg (shown in green) was visualized via indirect immunofluorescence staining using an inverted fluorescence microscope; nuclear DNA was counterstained with DAPI (blue). The merged images of the two stains are shown.



## Discussion

The effects of GST-HG141 on the *in vitro* assembly of the purified recombinant c-terminally truncated HBV core protein Cp150 [16,17] were studied with the fluorescence quenching assay, SEC and TAM. In the fluorescence quenching assay, GST-HG141 significantly accelerated Cp150 assembly, as was evident by quenching of the fluorescence signal with an  $EC_{50}$  value of  $0.93 \pm 0.11 \mu\text{M}$  (Mean  $\pm$  SD), confirming that GST-HG141 is a CAM. This conclusion was further confirmed by SEC. Treatment with  $30 \mu\text{M}$  GST-HG141 did not significantly change the retention time of the intact capsids (first peak), consistent with its CAM-E MOA, while BAY41-4109 (a known CAM-A), altered (shortened) the retention time of the first peak, as expected, suggesting formation of larger core protein aggregates. Next, the assembly of the Cp150 protein, with or without treatment with CAMs, was visualized by TEM. In these experiments, treatment with GST-HG141 did not cause apparent changes in capsid size or morphology (Figure 2), consistent with its CAM-E MOA, whereas treatment with GLS4 (CAM-A) led to formation of aberrant HBcAg structures, as expected. Thus, our results of the fluorescence quenching assay, SEC and TEM studies demonstrated that GST-HG141 accelerates *in vitro* assembly of the recombinant c-terminally truncated HBV core protein Cp150, but does not change the size or morphology of Cp150 capsids, consistent with the CAM-E MOA (formation of morphologically intact capsids, devoid of HBV genomes).

GST-HG141 potently inhibited secretion of HBV DNA in HepG2.2.15 cells in the absence of cytotoxicity. GST-HG141 also potently inhibited HBV isolates from other genotypes (A-D), showing broad-spectrum activity against most prevalent HBV genotypes globally [18]. In the same assay, GST-HG141 also retained potency against a number of major known CAM- and nucleos(t)ide-resistant mutants. GST-HG141 was not active *in vitro* against several tested representative DNA and RNA (plus- or minus-strand) viruses, suggesting its specificity towards HBV, as expected for HBV CAMs.

GST-HG141 appears to have a novel MOA distinct from other CAMs (CAM-E and CAM-A). In HepG2.1.15 cells, GST-HG141 significantly reduced both HBV DNA and HBV RNA content of the intracellular HBV capsids after a 7-day treatment with the drug (Figure 5). Intracellular core particles were resolved by native high-concentration agarose gel electrophoresis, followed by Western, Southern- and Northern blotting with HBV-specific antibodies and probes, as described in Materials and Methods. Treatment with  $1 \mu\text{M}$  ETV led to a drastic decrease in encapsidated viral DNA, and increase in RNA encapsidation, consistent with ETV being a nucleoside inhibitor of reverse transcription by HBV polymerase. No effect on capsid formation was observed with ETV, as expected. No core particles were observed after treatment with the reference CAM-A compound, GLS4, consistent with the TEM data (Figure 2) and with this drug MOA. Treatment with the reference CAM-E compound, AT-130 blocked DNA and RNA encapsidation and increased capsid formation, consistent with CAM-E MOA. A concentration-dependent shift from  $T = 4$  capsids to  $T = 3$  capsids was also observed with AT-130. This phenomenon was previously observed by others with AT-130 and other CAM-E, JNJ-56136379 [19]. Interestingly, this  $T = 4$  to  $T = 3$  capsids shift was not observed with GST-HG141. At lower concentrations ( $0.01$  and  $0.1 \mu\text{M}$ ) of GST-HG141, a dose-dependent decrease of both HBV DNA and RNA was observed, with dose-dependent increase in capsid formation. At  $0.1 \mu\text{M}$  of GST-HG-141, all core protein migrated as intact capsids, devoid of HBV DNA or RNA, fully consistent with CAM-E MOA. However, at higher concentrations of the drug ( $1 \mu\text{M}$ ), virtually no intact capsids were observed, and the core protein migrated as a heterogeneous larger aggregates (Figure 5). This effect is in line with CAM-E MOA, however, larger core aggregates, observed with GST-HG141, were not observed with AT-130, a CAM-E. These data suggest that the mechanism of capsid disruption by GST-HG141 may be different from that of AT-130, and possibly from other CAM-Es. Also, this observation of capsid disruption contrasts with our SEC and TEM data, showing that a recombinant c-terminally truncated

core protein Cp150 assembles into morphologically intact capsids in the presence of up to  $30 \text{ M}$  GST-HG141 (Figure 1-2).

These observations may indicate that the *in vitro* assembly of a purified recombinant assembly domain of HBcAg, widely used as a model for HBcAg assembly, may not fully represent all aspects of a full-length HBcAg assembly under physiological conditions. Taken together, our data suggest that treatment with GST-HG-141 at sub-micromolar concentrations leads to formation of morphologically-intact capsids, devoid of HBV genomes by a unique molecular mechanism of action differing from other CAM-Es (no  $T = 4$  to  $T = 3$  capsid shift). At higher concentrations, GST-HG141 may disrupt capsid formation, suggesting a possibility for additional mechanisms of HBV inhibition (e.g., disruption of the incoming HBV capsids in the cytoplasm after HBV cell entry). It has been reported previously that CAMs cause intracellular re-localization of the HBV core antigen (HBcAg), and this re-localization correlates with the CAMs effect on capsid assembly. While HAPs cause re-distribution of HBcAg from diffuse nucleoplasm to punctate nuclear structures (nuclear domains), all other known CAM classes, including SBA, PPA and dibenzo-thiazepin-2-one (DPT), led to re-distribution of HBcAg from the nucleoplasm to the cytoplasm [7]. We aimed to determine if GST-HG141 affects intracellular localization of HBcAg, and to compare it to the effect of known CAMs of different classes: GLS4 (HAP) and AT-130 (PPA). Untreated HepAD38 cells demonstrated typical HBcAg localization: predominantly diffuse nuclear (nucleoplasm), but also diffuse cytoplasmic (Figure 6A).

Treatment with  $0.1 - 10 \mu\text{M}$  AT-130 leads to a concentration-dependent re-distribution of HBcAg from the nucleoplasm to the cytoplasm (diffuse cytoplasmic staining) (Figure 6B). These observations were consistent with the previously published data [19]. Treatment with GLS4 led to redistribution of HBcAg within the nucleus: from the nucleoplasm (diffuse nuclear staining) to discrete nuclear domains (punctate nuclear pattern, (Figure 6C)). This finding was also in line with the previously published observations with GLS4 and other HAP CAMs [20]. The effect of GST-HG141 on the intracellular localization of HBcAg was similar to that observed with AT-130: re-distribution from predominantly diffused nuclear to predominantly diffused cytoplasmic localization (Figure 6D). This effect was already visible with  $0.01 \mu\text{M}$  GST-HG141, and was gradually enhanced with compound concentration increase up to  $10 \mu\text{M}$  (not shown).

The results of this experiments show that GST-HG141 had a pronounced effect on the intracellular localization of HBcAg in HepAD38 cells [21-23]. Treatment with GST-HG141, even at very low concentrations ( $0.01 \mu\text{M}$ ), led to re-distribution of HBcAg from the nucleus to the cytoplasm. This effect was concentration dependent. Similar effect was observed with AT-130, a CAM-E that belongs to the PPA class. In contrast, GLS4, a CAM-A from the HAP class, had a very different effect: it caused re-localization of HBcAg from the nucleoplasm to the nuclear domains, consistent with the published data [7]. Thus, the effect of GST-HG141 on the intracellular localization of HBcAg was similar to that of CAM-Es of SPA, PPA and DBT classes, suggesting that the MOA of GST-HG141 might resemble this class of CAMs: assembly of morphologically intact but lacking viral genome capsids [24].

To dissect the effect of GST-HG141 on different stages of HBV life cycle, HBV-infected PHHs were treated with HBV inhibitors in two different regimens: i) treatment started at the time of HBV infection (early treatment); or ii) treatment started at day 5 post-infection (late treatment). GST-HG141 potently and concentration-dependently inhibited the extracellular HBV DNA after either early or late treatment regimens. In contrast, the extracellular HBeAg, HBsAg and intracellular HBV cccDNA were inhibited after the early, but not the late treatment regimen. Similar results were observed for GLS4. As a nucleotide analog, ETV ( $5 \mu\text{M}$ ) potently inhibited extracellular HBV DNA upon both treatment regimens, but had no significant activity against extracellular HBeAg, HBsAg, and intracellular cccDNA for neither early nor late treatment regimens, as was expected for a reverse transcription inhibitor.



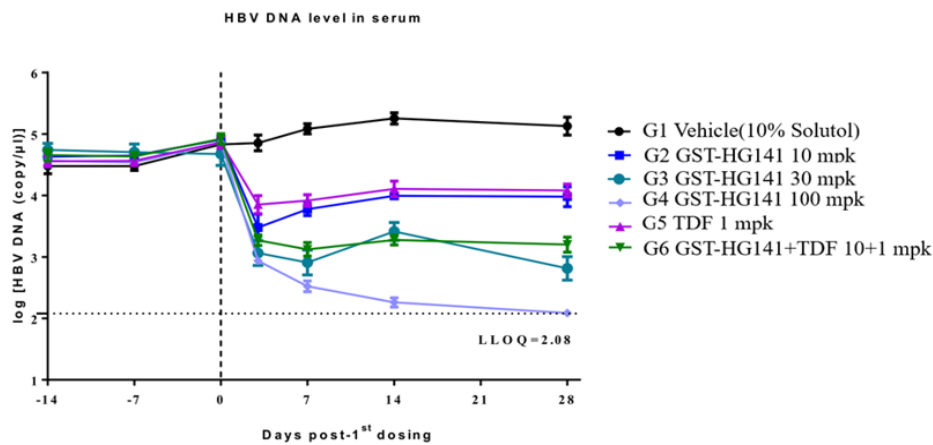


**Figure 7A** : Effect of GST-HG141 alone or in combination with TDF on serum HBV DNA levels in mouse AAV/HBV model. Male C57BL / 6 mice were injected with AAV / HBV (genotype D) plasmid DNA and, after 4 weeks, animals were administered by oral gavage with various doses of vehicle (BID), GST-HG141 (BID), or TDF (QD) for 28 days. The HBV DNA and HBV RNA in serum, as well as HBV DNA in the liver, was quantitated by the real-time qPCR.

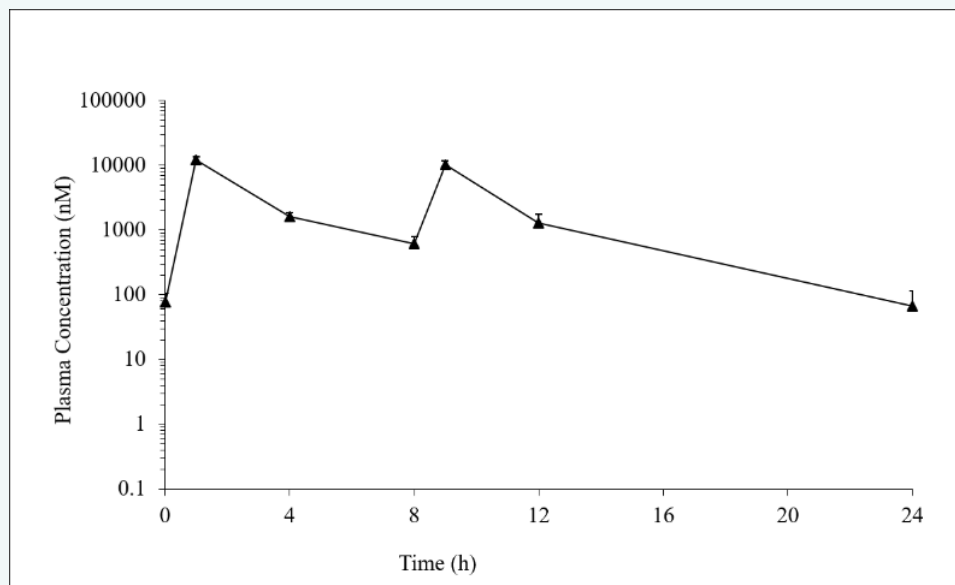


**Figure 7B**: Plasma drug concentration after oral BID administration of 10 mg/kg GST-HG141 to AAV/HBV mice.

These data suggest that GST-HG141 inhibits HBV replication in HBV-infected PHHs on the early stages of infection: post-entry, but before the HBV cccDNA is established in the nuclei. The inhibition of the cccDNA synthesis might occur via disruption of the incoming HBV capsids in the cytoplasm upon HBV entry, thus preventing transport of viral DNA into the nucleus. This assumption is in line with the observation that upon GST-HG141 treatment intracellular core protein is localized in the cytoplasm, and not in the nucleus (Figure 6). GST-HG141 has since entered Ph1 and Ph2 clinical development (data reported elsewhere).

GST-HG141 demonstrated excellent safety and tolerability, as well as dose proportional PK characteristics in healthy Chinese subjects in phase 1a study (NCT04386915) [9]. In multiple ascending-dose 28-day phase Ib study in CHB patients (NCT04868981), a rapid and robust decline in serum HBV DNA was observed (median 2.9 and 3.4 log<sub>10</sub> IU/ml for 50 and 100 mg dose cohorts, respectively). HBV DNA rebound occurred in 5 days after drug withdrawal accordingly, but the rebound rate was lower in high-dose cohort. The HBV pgRNA levels also decreased by median 2.37 log<sub>10</sub> IU/ml in 100 mg dose cohorts [10]. These clinical observations are



comparable with, or superior to the clinical results with other CAMs, and are consistent with our preclinical MOA studies presented here. A phase II clinical study with a combo of GST-HG141 and nucleoside analogs is currently underway.

In summary, GST-HG141 demonstrated novel MOA and preclinical profile compared to other HBV CAMs. Collectively, the data suggest that GST-HG141 induces the formation of morphologically intact viral capsids, devoid of viral genetic material ("empty" capsids), and acts on different steps of the HBV life cycle with a novel mechanism distinct from other CAMs. GST-HG141 exhibited potent antiviral activities in HBV-replicating cell line, human primary hepatocytes (PHHs), and AAV/HBV mouse model. Moreover, GST-HG141 retained potent antiviral activity against HBV genotypes A-D, and nucleos(t)ide- and CAM-resistant mutants with additive effect with nucleos(t)ide inhibitors. These properties support that GST-HG141 is being further developed as a potential novel CHB treatment.

10. Mai J, Zhang H, Wu M, Ding Y, Niu J, Bichko VV, et al. Safety, pharmacokinetics and antiviral activity of GST-HG141, a hepatitis B virus capsid assembly modulator, in subjects with chronic hepatitis B. 2022.
11. Stray SJ, Zlotnick A. BAY 41-4109 has multiple effects on Hepatitis B virus capsid assembly. *J Mol Recognit.* 2006; 19(6): 542-548. doi: 10.1002/jmr.801. PMID: 17006877.
12. Zlotnick A, Cheng N, Conway JF, Booy FP, Steven AC, Stahl SJ, Wingfield PT. Dimorphism of hepatitis B virus capsids is strongly influenced by the C-terminus of the capsid protein. *Biochemistry.* 1996; 35(23): 7412-7421. doi: 10.1021/bi9604800. PMID: 8652518.
13. Zlotnick A, Cheng N, Stahl SJ, Conway JF, Steven AC, Wingfield PT. Localization of the C terminus of the assembly domain of hepatitis B virus capsid protein: implications for morphogenesis and organization of encapsidated RNA. *Proc Natl Acad Sci U S A.* 1997; 94(18): 9556-9561. doi: 10.1073/pnas.94.18.9556. PMID: 9275161; PMCID: PMC23216.
14. Stray SJ, Bourne CR, Punna S, Lewis WG, Finn MG, Zlotnick A. A heteroaryl dihydropyrimidine activates and can misdirect hepatitis B virus capsid assembly. *Proc Natl Acad Sci U S A.* 2005; 102(23): 8138-8143. doi: 10.1073/pnas.0409732102. Epub 2005 May 31. PMID: 15928089; PMCID: PMC1149411.
15. Schlicksup CJ, Wang JC, Francis S, Venkatakrishnan B, Turner WW, VanNieuwenhze M, et al. Hepatitis B virus core protein allosteric modulators can distort and disrupt intact capsids. *Elife.* 2018; 7: e31473. doi: 10.7554/eLife.31473. PMID: 29377794; PMCID: PMC5788503.
16. Zoulim F, Zlotnick A, Buchholz S, Donaldson E, Fry J, Gaggar A, et al. Nomenclature of HBV core protein-targeting antivirals. *Nat Rev Gastroenterol Hepatol.* 2022; 19(12): 748-750. doi: 10.1038/s41575-022-00700-z. PMID: 36207612; PMCID: PMC10442071.
17. Sunbul M. Hepatitis B virus genotypes: global distribution and clinical importance. *World J Gastroenterol.* 2014; 20(18): 5427-5434. doi: 10.3748/wjg.v20.i18.5427. PMID: 24833873; PMCID: PMC4017058.
18. Berke JM, Dehertogh P, Vergauwen K, Mostmans W, Vandyck K, Raboisson P, et al. Antiviral Properties and Mechanism of Action Studies of the Hepatitis B Virus Capsid Assembly Modulator JNJ-56136379. *Antimicrob Agents Chemother.* 2020; 64(5): e02439-19. doi: 10.1128/AAC.02439-19. PMID: 32094138; PMCID: PMC7179615.
19. Terrault NA, Lok ASF, McMahon BJ, Chang KM, Hwang JP, Jonas MM, et al. Update on prevention, diagnosis, and treatment of chronic hepatitis B: AASLD 2018 hepatitis B guidance. *Hepatology.* 2018; 67(4): 1560-1599. doi: 10.1002/hep.29800. PMID: 29405329; PMCID: PMC5975958.
20. Hirt B. Selective extraction of polyoma DNA from infected mouse cell cultures. *J Mol Biol.* 1967; 26(2): 365-369. doi: 10.1016/0022-2836(67)90307-5. PMID: 4291934.
21. Zhou T, Guo H, Guo JT, Cuconati A, Mehta A, Block TM. Hepatitis B virus e antigen production is dependent upon covalently closed circular (ccc) DNA in HepAD38 cell cultures and may serve as a cccDNA surrogate in antiviral screening assays. *Antiviral Res.* 2006; 72(2): 116-124. doi: 10.1016/j.antiviral.2006.05.006. Epub 2006 Jun 2. PMID: 16780964.



22. Cai D, Nie H, Yan R, Guo JT, Block TM, Guo H. A southern blot assay for detection of hepatitis B virus covalently closed circular DNA from cell cultures. *Methods Mol Biol.* 2013; 1030: 151-161. doi: 10.1007/978-1-62703-484-5\_13. PMID: 23821267; PMCID: PMC5060941.
23. Niu C, Livingston CM, Li L, Beran RK, Daffis S, Ramakrishnan D, et al. The Smc5/6 Complex Restricts HBV when Localized to ND10 without Inducing an Innate Immune Response and Is Counteracted by the HBV X Protein Shortly after Infection. *PLoS One.* 2017; 12(1): e0169648. doi: 10.1371/journal.pone.0169648. PMID: 28095508; PMCID: PMC5240991.
24. Ladner SK, Otto MJ, Barker CS, Zaifert K, Wang GH, Guo JT, et al. Inducible expression of human hepatitis B virus (HBV) in stably transfected hepatoblastoma cells: a novel system for screening potential inhibitors of HBV replication. *Antimicrob Agents Chemother.* 1997 Aug; 41(8): 1715-1720. doi: 10.1128/AAC.41.8.1715. PMID: 9257747; PMCID: PMC163991.